Understanding Mechanical Properties of Nano-Grained Bainitic Steels from Multiscale Structural Analysis

Francisca G. Caballero [1,*], Rosalia Rementeria [1,2], Lucia Morales-Rivas [1,3],
Miguel Benito-Alfonso [1], Jer-Ren Yang [4], David de Castro [1], Jonathan D. Poplawsky [5],
Thomas Sourmail [6] and Carlos Garcia-Mateo [1]

[1] Department of Physical Metallurgy, National Center for Metallurgical Research (CENIM-CSIC), Avda Gregorio del Amo, 8; Madrid, E-28040, Spain; rosalia.rementeria@arcelormittal.com (R.R.); rivas@mv.uni-kl.de (L.M.-R.); miguelba46@gmail.com (M.B.-A.); david.decastro@cenim.csic.es (D.d.C.); cgm@cenim.csic.es (C.G.-M.)

[2] ArcelorMittal, SLab—Steel Labs: Global R&D, Calle Marineros, 4, 33490 Avilés, Asturias, Spain

[3] Materials Testing, University of Kaiserslautern, Gottlieb-Daimler-Straße, 67663 Kaiserslautern, Germany

[4] Department of Materials Science and Engineering, National Taiwan University, 1, Roosevelt Rd. Sec. 4, Taipei, Taiwan; jryang@ntu.edu.tw

[5] Center for Nanophase Materials Sciences, Oak Ridge National Laboratory, PO Box 2008 MS6064, Oak Ridge, TN 37831-6064, USA; poplawskyjd@ornl.gov

[6] Metallurgy Department, Asco Industries Research (CREAS), BP 70045 Hagondange, France; thomas.sourmail@ascometal.com

* Correspondence: fgc@cenim.csic.es; Tel.: +34-915-53-89-00

Abstract: Steel components working in extreme conditions require materials presenting the highest performances. Nowadays, nanoengineering is being applied to the development of ultra-high strength steels as a key-enabling technology in the steel sector. The present article describes the multiscale structure of nano-grained steels designed using atomic transformation theory and processed by a simple heat treatment. Outstanding mechanical properties for these novel steels are reported, and strain-hardening mechanisms are discussed.

Keywords: steel; bainite; ultra-high strength; ductility; in-use properties

1. Nano-Grained Steels Formed by Solid Reaction

Reducing the grain size is the most common approach to improving the strength of polycrystalline materials. The reason is that the finer the grain size, the more quantity of grain boundary per unit volume of material, and thus the more difficult for dislocations to slide [1]. Thermomechanical processes, heat treatments or alloying additions are the traditional strategies to produce ultra-fine grained metals (100 nm–1 μm) [2], whereas deposition-based processes and severe plastic deformation processes ensure the nanocrystallization (<100 nm) of metal structures [3,4].

In steels, it is also possible to heavily refine ferritic crystals by promoting displacive transformations at low temperatures or by rapid cooling [5]. Ultra-fine needle-shaped ferrite crystallites, as in martensite and bainite, grow by displacive transformation, while polygonal ferrite, coarse-grain boundary allotriomophs and intragranular idiomorphs, are formed by a reconstructive mechanism [6].

Displacive reactions involve a sudden, ordered movement of iron atoms, which is accompanied by a given crystal correspondence between the austenite and ferrite lattices, and a macroscopic shape

strain of the transformed structure [7]. Ferrite, in displacive transformation products, is formed as ultra-fine plate-like structures to minimize the large elastic strain energy [8]. It also applies to bainite, where the shape change is partially accommodated by plastic deformation, and the introduced defects limit the final size of formed plates, becoming thinner at low temperatures when the austenite is harder [9].

Applying these fundamental concepts and reducing bainite reaction temperatures drastically by high-carbon (0.6–1.0 wt.%) and high-silicon (1.5–3.0 wt.%) alloying additions [10], industrial components with bainitic structures consisting of nano-scale plates of ferrite and retained austenite, were manufactured by a simple isothermal heat treatment at low temperatures (125–325 °C), using dry gas technology for small components (20 cm × 2 cm × 3 cm) and a conventional salt bath for large components (70 cm × 40 cm × 20 cm) [11]. Preliminary tensile tests in lab cast material showed a remarkable combination of strength and ductility (Ultimate Tensile Strength) UTS, of 2075 MPa and total elongation of 20%) for samples containing 1.0 wt.% C and 3 wt.% Si additions and transformed at 250 °C, independent of the manufacturing route [12]. Development and upscaling of nano-grained bainitic steels (detailed compositions are given in Table 1) showed an outstanding wear performance and competitive values for fatigue strength [13].

Table 1. Chemical composition of nano-grained bainitic steels, wt.%. [10].

Steel		C	Si	Mn	Cr	Mo	V	Nb	Co	Al
First Generation	Nanobain 1	0.79	1.59	1.94	1.33	0.30	0.11	-	-	-
	Nanobain 2	0.83	1.57	1.98	1.02	0.24	-	-	1.54	-
	Nanobain 3	0.78	1.49	1.95	0.97	0.24	-	-	1.60	0.99
Second Generation	Nanobain 4	0.99	1.58	0.76	0.45	-	-	-	-	-
	Nanobain 5	1.00	1.53	0.75	0.51	-	-	0.02	-	-
	Nanobain 6	1.01	1.51	0.82	0.46	0.10	-	-	-	-
	Nanobain 7	0.98	2.90	0.77	0.45	-	-	-	-	-
	Nanobain 8	0.88	1.54	0.69	0.50	-	-	-	-	-
	Nanobain 9	0.67	1.60	1.25	1.50	-	-	-	-	-
	Nanobain 10	0.61	1.45	0.76	2.42	-	-	-	-	-
	Nanobain 11	0.64	1.60	1.27	1.50	-	-	0.03	-	-
	Nanobain 12	0.58	1.63	1.29	1.43	0.1	-	-	-	-

The aim of the present work is to outline the multiscale complexity of nano-grained bainitic structures, revealing their intricate-phase distribution and carbon accumulation at the nearly atomic scale. For that purpose, a wide variety of techniques, including scanning and transmission electron microscopy (SEM and TEM), X-ray diffraction analysis (XRD), atom-probe tomography (APT) and electron backscatter diffraction (EBSD), has been used. The rationalization to their unprecedented mechanical performances was possible only after the comprehensive examination of the structure at several length scales.

2. Complex Composite-Like Structures

Figure 1 illustrates, at different magnifications, bainitic structures formed at low temperature in high-carbon high-silicon steels. They are revealed as a complex composite-like structure of two phases, ferrite (α) and austenite (γ). According to XRD, these bainitic structures can contain a significant amount of austenite (25–50%), depending on the transformation processes. While plates of ferrite are some tens of nanometers thick, austenite is retained in the ferritic matrix as two very different shapes, thin films between the plates of ferrite, also in the nanoscale, and coarser austenite blocks, in the micro and sub-micron scale as the SEM image in Figure 1a illustrates.
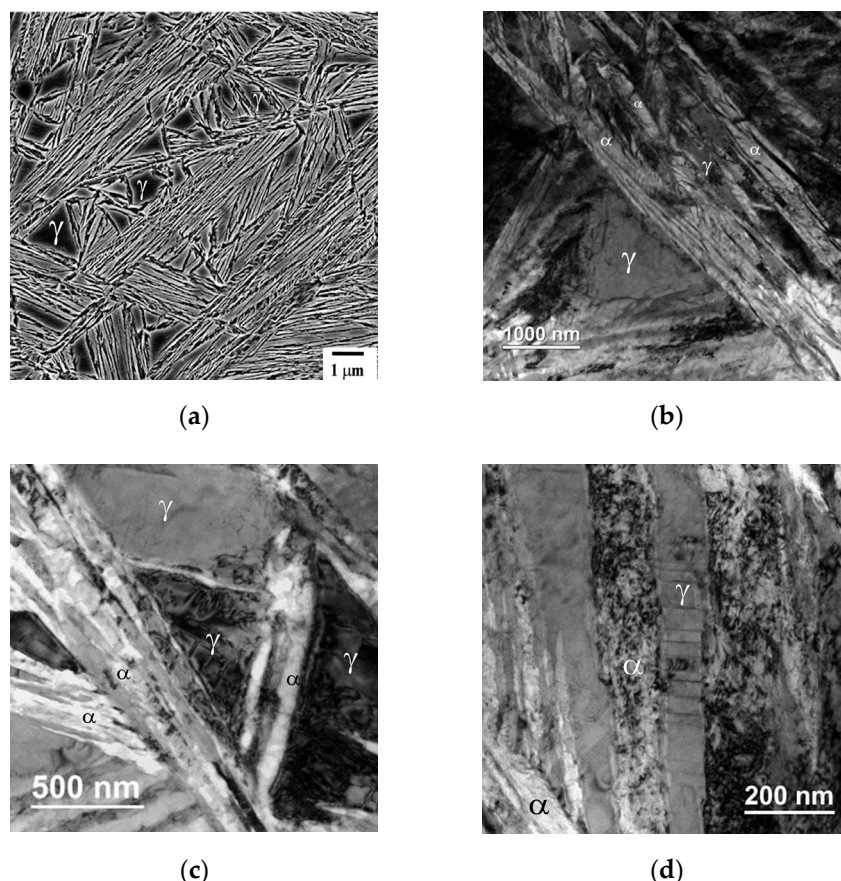
Figure 1. (**a**) SEM and (**b**–**d**) TEM images of bainite formed at 220 °C for 22 h in a high-carbon (1.0 wt.%) and high-silicon (2.5 wt.%) steel; α is bainitic ferrite, and γ is retained austenite.

Although the bainite reaction is controlled by a diffusionless growth process, the supersaturation of carbon within ferrite is rapidly reduced by carbon partitioning into the residual austenite [14]. Here, silicon addition inhibits the precipitation of cementite from austenite, and then carbon-enriched austenite is stabilized in the structure by the local suppression of the martensite start temperature. Given their morphological constraints and their specific location in the structure, thin films of austenite trapped between bainitic ferrite plates contain higher carbon than blocks of austenite [15]. As a result, high-silicon bainitic steels can contain an intricate carbon distribution in austenite with different morphologies and a wide range of austenitic grain sizes [12].

The high density of defects generated by plastic relaxation in austenite during the displacive reaction is apparently close to the austenite/ferrite interface in TEM images (Figure 1b,c). At the exact-zone diffraction condition of austenite, in addition to dislocations' tangles, multiple planar faults/twins in films of austenite are clearly observed; see Figure 1d [16]. Carbon might also segregate at these defects, therefore, interfering in the carbon-partitioning process into austenite after ferrite formation [17].

At low-transformation temperatures, part of the carbon in the ferritic structure has the opportunity to precipitate inside the bainitic ferrite plates [18]. According to TEM images in Figure 1, cementite particles are not observable as in the classical lower bainite. APT [19] and, more recently, in-situ synchrotron high energy XRD [20] have revealed the presence of cementite and η-carbide in low temperature bainite. Figure 2 illustrates the fine-carbon distribution detected in bainitic ferrite as a result of bainite reaction at 220 °C in a high-carbon high-silicon steel. Particles with an apparent carbon content of about 25 wt.% are identified as cementite [21].

APT solute atom maps and corresponding proximity histograms in Figure 2 also quantify the redistribution of substitutional-solute partitioning across the interface, with special attention given to silicon. As already mentioned, silicon additions avoid the precipitation of carbides from austenite

between the plates of bainitic ferrite, but it does not have an effect on the precipitation of carbides inside the ferrite plates. Evidences in Figure 2 confirm cementite precipitation within bainitic ferrite in high-silicon steels. The absence of partitioning of silicon, or other substitutional elements in APT results, suggest that cementite grows under paraequilibrium conditions [16].
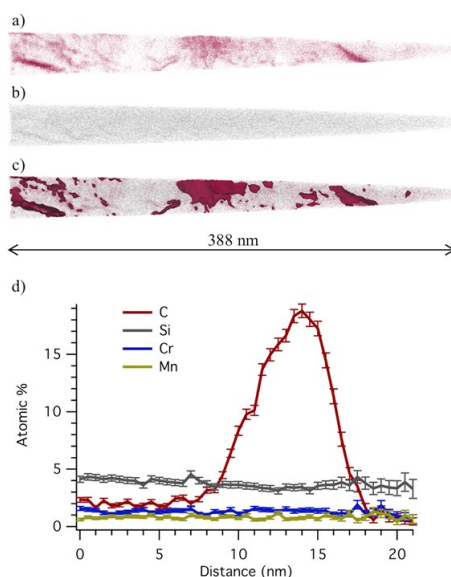

Figure 2. (**a**) Carbon and (**b**) silicon atom maps, (**c**) carbon isoconcentration surfaces at 5 wt.% C, and (**d**) proximity histogram across cementite plate in bainitic ferrite after transformation at 220 °C for 24 h in a high-carbon (0.7 wt.%) and high-silicon (1.5 wt.%) steel.

In displacive reactions, the transformation product is restricted to the parent grain, and ferrite is formed with a crystal correspondence, in between the classic Kurdjumov-Sachs (K-S) and Nishiyama-Wassermann (N-W) orientation relationships. As the inverse-pole figure color map images in Figure 3 illustrate, low-temperature bainite exhibits the hierarchy ferritic sub-structure of blocks, i.e., aggregates of plates of ferrite of equal variant or variants slightly misoriented, and packets, i.e., adjacent blocks with a {1 1 0} ferrite plane almost parallel to the same {1 1 1} austenite plane, which is characteristic of lath martensite and bainitic ferrite in low-carbon steel [22–24]. The colors correspond to a crystal orientation, normal to the observed plane, representing different crystallographic variants. Here, a prior austenite grain encloses packets formed by three blocks with different orientations, and each block contains a single variant of ferrite.
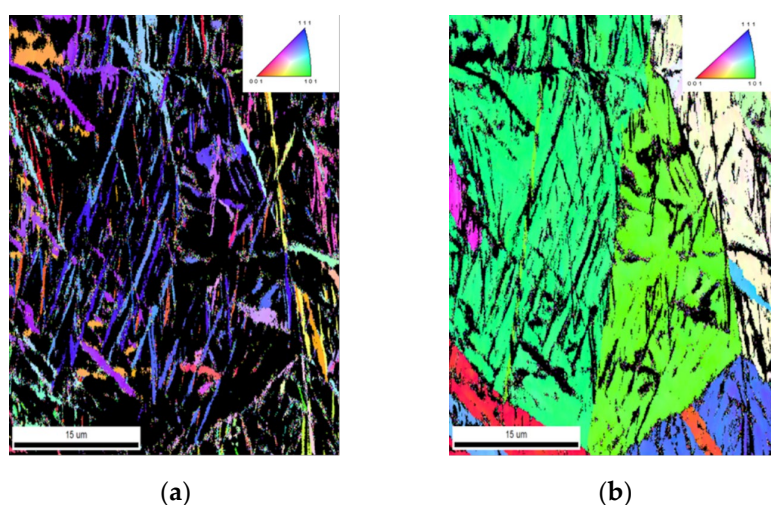

(**a**)　　　　　　　　　　　　　　　　　　　(**b**)

Figure 3. Electron backscatter diffraction (EBSD) orientation maps of the structure formed at 220 °C for 22 h in a high-carbon (1.0 wt.%) and high-silicon (2.5 wt.%) steel: (**a**) indexed ferrite is shown; (**b**) indexed austenite is shown.

3. Understanding Tensile Properties of Nano-Grained Bainitic Steels

Exceptional hardness values (up to 700 HV), ultra-high strength values (up to 2 GPa) and, in some cases, unprecedented total elongations of more than 20% have been reported in low-temperature bainite [12]. The strength in these structures comes from the high fraction of nano-scale ferritic plates, the high density of defects and the complex carbon distribution observed by atom-probe tomography and illustrated in Figure 2 [10]. What is remarkable is that, in addition to the nano-scale refinement of the structure, these steels are homogeneous in terms of Young's modulus [25]. This fact, together with a similar strength of the hard-bainitic ferrite and the carbon-enriched austenite, ensures under loading a low-stress partitioning between the phases [26], which is key to achieve large elongations.

In addition, retained austenite may transform under deformation to martensite as TEM images show, in Figure 4. The formation of twinned martensite in nano-grained bainite subjected to 6.4% deformation is confirmed by the diffraction pattern. The mechanical stability of austenite, i.e., its ability to remain untransformed during deformation, is mainly governed by its local chemical composition, its shape and size, crystal texture and the local constraint of the surrounding ferritic matrix [27].
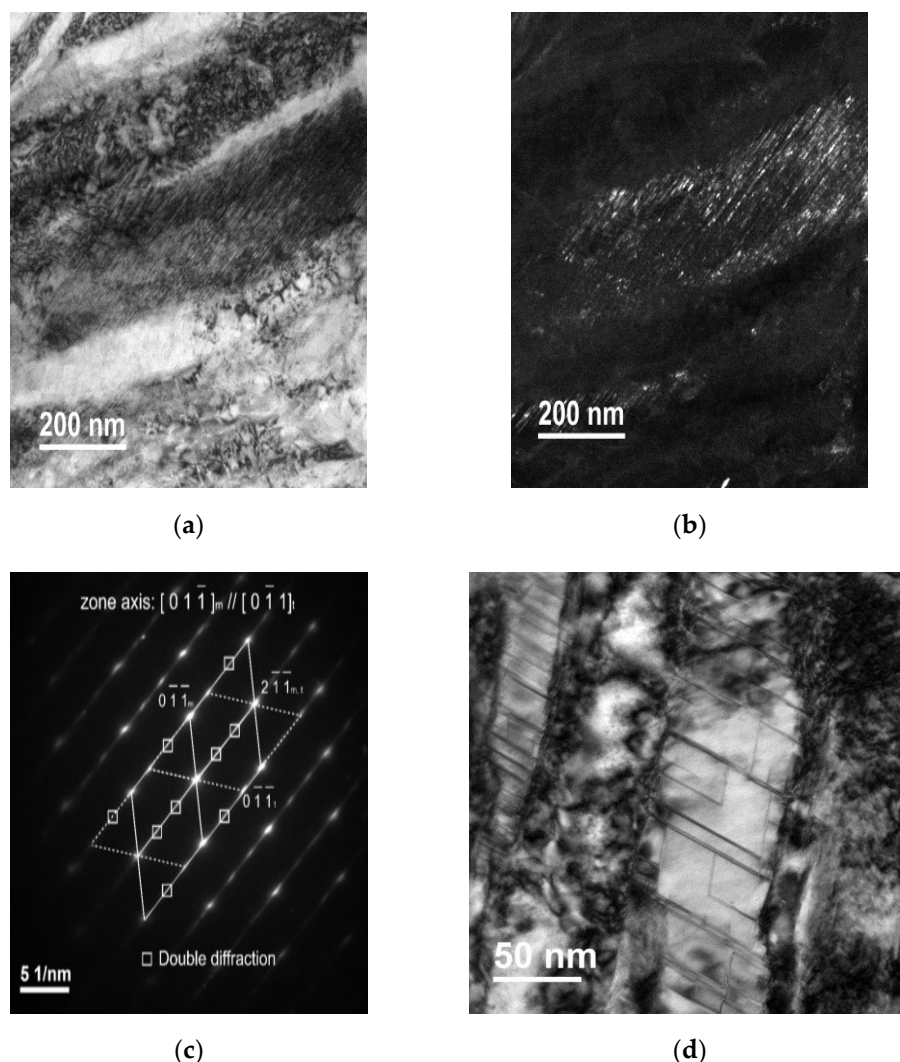
(**a**)

(**b**)

(**c**)

(**d**)

Figure 4. (**a**) Bright and (**b**) dark field TEM images, and (**c**) corresponding diffraction pattern, of twinned martensite in bainite formed at 220 °C for 22 h and deformed up to 2% strain in a high-carbon (1.0 wt.%) and high-silicon (2.5 wt.%) steel. (**d**) Bright field micrograph of mechanical twins in austenite in the same bainitic structure deformed up to 6% strain.

Likewise, plastic deformation prior to mechanically-induced martensitic transformation is necessary to reach optimum uniform elongations in nano-grained bainitic steels. With the help of in-situ neutron diffraction analysis [26] during tensile testing at room temperature, it was found that rapid strain hardening and, thus, premature failure is related to local stress-induced transformation of austenite to martensite, which is promoted by the constraint of stronger bainitic ferrite. On the contrary, when both ferrite and austenite consistently deform, larger elongations are achieved.

Additionally, the formation of twins in austenite films has been identified as a strain-hardening mechanism, contributing to ductility in these structures [28]. TEM examination of deformed structures revealed that thin films of austenite contained twins, and some of these twins are considered to be accommodation twins from the displacive transformation as those observed in undeformed samples and shown in Figure 1d; but, also a second variant of twinning was observed in deformed samples with a high-strain level. Mechanical twins in austenite were formed by the direct effect of the stress. This is illustrated in a TEM image in Figure 4d. Since the local carbon content in austenite has a direct influence on the local-activated strain mechanisms, the austenite-twinning-induced plasticity (TWIP) effect, as well as the austenite-to-martensite transformation-induced plasticity (TRIP) effect, is possible in these structures by tailoring the carbon distribution in austenite with different morphologies and a wide range of austenitic grain sizes.

4. In-Use Properties and Application of Nano-Grained Bainite

The commercial prospective of nano-grained bainite is vast because the steels are processed by conventional treatments [11,13]. However, before industrialization, complex properties, such as wear resistance, toughness and fatigue endurance, have to be examined.

Two types of wear experiments, sliding/rolling wear resistance and high-pressure abrasive wear resistance, were performed to study the behavior of the nanoscale bainite under different working conditions [29]. Outstanding wear performance was detected on reciprocating sliding tests compared to ultra-fine bainitic structures of equal or similar hardness. The highly refined structure and the transformation under strain of the austenite films contributed to the surface hardening, improving the wear performance [30].

The high-pressure abrasive wear resistance was studied in conjunction with Charpy V impact toughness tests [11]. The performance of nanostructured bainite in these tests was found to be on par with significantly more expensive alloys, such as Hardox 500, which is a medium carbon, medium silicon commercial steel heat treated to a hardness of 500 HV; and largely improved, compared to 100Cr6 steel transformed to bainite.

Regarding rotation-bending fatigue, nano-grained bainite appeared to exhibit similar or lower fatigue strength, compared to 100Cr6 in spite of somewhat lower UTS [13]. However, the presence of retained austenite might be playing an important role on fatigue [31]. Microstructural examination by EBSD below the fracture surface enabled the identification of the nature of boundaries deflecting the crack [32]. Results confirmed that crystal boundaries, between separating bainite blocks, packets and twins, are the most effective boundaries. In addition, the block size was identified as the structure's parameter controlling crack propagation. Unfortunately, the effect of austenite morphology and distribution on the fatigue strength of these structures is uncertain mainly due to the technical difficulties of EBSD indexing this phase embedded in a nano-grained structure [32].

The stability of nano-grained bainitic structures between 300 °C and 750 °C was investigated using XRD, TEM and APT [33,34]. After tempering at 300 °C and 400 °C, a negligible change in the initial microstructure is observed. However, by increasing the tempering temperature to 450 °C, the austenite films decomposed into cementite and ferrite, though the austenite blocks persisted in the microstructure. This is because the films of austenite are much more enriched in carbon and, therefore, have a higher driving force for cementite precipitation.

Further decomposition of retained austenite occurs as temperature increases, and some large regions of retained austenite transform into colonies of pearlite with a fine interlamellar spacing. Tempering temperatures of 500 °C and above lead to microstructures where austenite is no longer observed but substituted by ferrite and carbides; the higher the tempering temperature, the coarser

the carbides. Ferrite plate morphology still remains after tempering at 550 °C. However, there is a significant reduction in hardness at 600 °C, due to coarsening of the ferritic structure.

Recently, a group of steel makers, end-users and researchers has explored the application of these structures under different industrial settings, such that the appropriate alloy was chosen for each application and its performance was evaluated through industrial or semi-industrial trials [35]. They have questioned if outstanding preliminary results in rolling-sliding conditions can also be achieved in other wear-based applications and in contact fatigue, where former studies were not so conclusive. They confirmed that nano-grained steels perform very well in applications, related to contact fatigue, or contact fatigue combined with some sliding wear, but they did not provide an advantage in applications related to third-body abrasion or abrasive wear.

Out of the studied industrial applications, high-carbon high-silicon bainitic steels have showed competitive performance on bearings, on steel mill rollers, especially for warm application, i.e., as guide rollers, and on sheet metal, cutting punches over the reference X153CrMoV12 steel sandblasted and coated. Interestingly, nano-grained bainitic steels also performed well as coating substrate. In that case, the application of a hard coating decreased the amount of abrasive wear suffered, while the good contact fatigue resistance avoided the appearance of chipping or cracking.

5. Conclusions

Recently developed innovative ultra-high strength steels rely on nano-grained bainitic structures, which contain a significant amount of austenite (25–50%), depending on the transformation processes. The ferrite matrix is heavily dislocated and hierarchically sub-structured into packets, blocks and laths as a natural consequence of the atomic displacive transformation mechanisms. In addition, the austenite is present in two forms: (i) micron/submicron blocks of retained austenite located between the ferrite packets and (ii) nano-scale films of austenite, which are retained between the ferrite lath subunits within a given packet or block. The retained austenite may transform into martensite during deformation, which enables ultra-high-strength steels to reach unprecedented uniform elongations. However, other strain mechanisms, such as twinning in austenite, cannot be excluded; in fact, twinning can be activated locally in an austenite region of these novel structures with a preference for certain morphology and austenite grain sizes based on its composition.

Author Contributions: conceptualization, F.G.C. and T.S.; materials and treatments, T.S.; EBSD analysis, R.R. and L.M.-R.; TEM examination, M.B.-A. and J.-R.Y.; APT analysis, D.d.C., J.D.P.; Strengthening analysis, C.G.-M. and F.G.C.; in-use properties, R.R. and L.M.-R.; and writing—review and editing, F.G.C.

References

1.　Zlateva, G.; Martinova, Z. *Microstructure of Metals and Alloys*; CRC Press: Boca Raton, FL, USA, 2008; pp. 19–25.
2.　Humphreys, F.J.; Prangnell, P.B.; Priestner, R. Fine-grained alloys by thermomechanical processing. *Curr. Opin. Solid State Mater. Sci.* **2001**, *5*, 15–21.
3.　Erb, U.; Palumbo, G.; McCrea, J.L. The processing of bulk nanocrystalline metals and alloys by electrodeposition. In *Nanostructured Metals and Alloys: Processing, Microstructure, Mechanical Properties and Applications*, Whang, S.H., Ed.; Woodhead Publishing Limited: Oxford, UK, 2011; pp. 118–151.

4. Valiev, R.Z. Producing bulk nanostructured metals and alloys by severe plastic deformation (SPD). In *Nanostructured Metals and Alloys: Processing, Microstructure, Mechanical Properties and Applications*, Whang, S.H., Ed.; Woodhead Publishing Limited: Oxford, UK, 2011; pp. 3–39.

5. Krauss, G. *Steels, Processing, Structure and Performance*, 2nd ed.; ASM International: Materials Park, OH, USA, 2005; 63–67.

6. Bhadeshia, H.K.D.H.; Honeycombe, R. *Steels: Microstructure and Properties*, 4th ed.; Butterworths-Heinemann (Elsevier): London, UK, 2017; 59–100.

7. Christian, J.; Olson, G.; Cohen, M. Classification of displacive transformations: What is a martensitic transformation?. *J. Phys. IV* **1995**, *5*, C8-3–C8-10.

8. Christian, J.W. Accommodation strains in martensite formation, and the use of a dilatation parameter. *Acta Metall.* **1958**, *6*, 377–379.

9. Chang, L.C.; Bhadeshia, H.K.D.H. Metallographic observations of bainite transformation mechanism. *Mater. Sci. Technol.* **1995**, *11*, 105–108.

10. Caballero, F.G.; Garcia-Mateo, C.; Miller, M.K. Design of novel bainitic steels: Moving from ultrafine to nanoscale structures. *JOM* **2014**, *66*, 747–755.

11. Garcia-Mateo, C.; Sourmail, T.; Caballero, F.G.; Smanio, V.; Kuntz, M.; Ziegler, C.; Leiro, A.; Vuorinen, E.; Elvira, R.; Teeri, T. Nanostructured steel industrialisation: plausible reality. *Mater. Sci. Tech.* **2014**, *30*, 1071–1078.

12. Garcia-Mateo, C.; Caballero, F.G.; Sourmail, T.; Kuntz, M.; Cornide, J.; Smanio, V.; Elvira, R. Tensile behaviour of a nanocrystalline bainitic steel containing 3 wt% silicon. *Mater. Sci. Eng. A* **2012**, *549*, 185–192.

13. Sourmail, T.; Caballero, F.G.; Garcia-Mateo, C.; Smanio, V.; Ziegler, C.; Kuntz, M.; Elvira, R.; Leiro, A.; Vuorinen, E.; Teeri, T. Evaluation of potential of high Si high C steel nanostructured bainite for wear and fatigue applications. *Mater. Sci. Tech.* **2013**, *29*, 1166–1173.

14. Bhadeshia, H.K.D.H.; Christian, J.W. Bainite in steels. *Metall. Trans. A* **1990**, *21*, 767–797.

15. Caballero, F.G.; Garcia-Mateo, C.; Santofimia, M.J.; Miller, M.K.; Garcia de Andres, C. New experimental evidence on the incomplete transformation phenomenon in steel. *Acta Mater.* **2009**, *57*, 8–17.

16. Bhadeshia, H.K.D.H.; Edmonds, D.V. The bainite transformation in a silicon steel. *Metall. Trans. A* **1979**, *10*, 895–907.

17. Caballero, F.G.; Yen, H.-W.; Miller, M.K.; Yang, J.-R.; Cornide, J.; Garcia-Mateo, C. Complementary use of transmission electron microscopy and atom probe tomography for the examination of plastic accommodation in nanocrystalline bainitic steels. *Acta Mater.* **2011**, *59*, 6117–6123.

18. Takahashi, M.; Bhadeshia, H.K.D.H. A model for the transition from upper to lower. Bainite. *Mater. Sci. Tech.* **1990**, *6*, 592–603.

19. Caballero, F.G.; Miller, M.K.; Garcia-Mateo, C. Influence of transformation temperature on carbide precipitation sequence during lower bainite formation. *Mater. Chem. Phys.* **2014**, *146*, 50–57.

20. Rementeria, R.; Jimenez, J.A.; Allain, S.Y.P.; Geandier, G.; Poplawsky, J.D.; Guo, W.; Urones-Garrote, E.; Garcia-Mateo, C.; Caballero, F.G. Quantitative assessment of carbon allocation anomalies in low temperature bainite. *Acta Mater.* **2017**, *133*, 333–345.

21. Miller, M.K.; Beaven, P.A.; Brenner, S.S.; Smith, G.D.W. An atom probe study of the aging of iron-nickel-carbon martensite. *Metall. Trans. A* **1983**, *14*, 1021–1024.

22. Morito, S.; Tanaka, H.; Konishi, R.; Furuhara, T.; Maki, T. The morphology and crystallography of lath martensite in Fe-C alloys. *Acta Mater.* **2003**, *51*, 1789–1799.

23. Takayama, N.; Miyamoto, G.; Furuhara, T. Effects of transformation temperature on variant pairing of bainitic ferrite in low carbon steel. *Acta Mater.* **2012** *60*, 2387–2396.

24. Beladi, H.; Adachi, Y.; Timokhina, I.; Hodgson, P.D. Crystallographic analysis of nanobainitic steels. *Scr. Mater.* **2009**, *60*, 455–458.

25. Morales-Rivas, L.; González-Orive, A.; Garcia-Mateo, C.; Hernández-Creus, A.; Caballero, F.G.; Vázquez, L. Nanomechanical characterization of nanostructured bainitic steel: Peak force microscopy and nanoindentation with AFM. *Sci. Rep.* **2015**, *5*, 17164.

26. Babu, S.S.; Vogel, S.; Garcia-Mateo, C.; Clausen, B.; Morales-Rivas, L.; Caballero, F.G.; Microstructure evolution during tensile deformation of a nanostructured bainitic steel *Scr. Mater.* **2013**, *69*, 777–780.

27. Jacques, P.J. Transformation-induced plasticity for high strength formable steels. *Curr. Opin. Solid State Mater. Sci.* **2004**, *8*, 259–265.

28. Morales-Rivas, L.; Archie, F.; Zaefferer, S.; Benito-Alfonso, M.; Tsai, S.-P.; Yang, J.-R.; Raabe, D.; Garcia-Mateo, C.; Caballero, F.G. Crystallographic examination of the interaction between texture evolution, mechanically induced martensitic transformation and twinning in nanostructured bainite. *J. Alloy Compd.* **2018**, *752*, 505–519.

29. Leiro, A.; Vuorinen, E.; Sundin, K.-G.; Prakash, B.; Sourmail, T.; Smanio, V.; Caballero, F.G.; Garcia-Mateo, C.; Elvira, R.; Wear of nano-structured carbide-free bainitic steels under dry rolling-sliding conditions. *Wear* **2013**, *42*, 298–299.

30. Rementeria, R.; García, I.; Aranda, M.M.; Caballero, F.G. Reciprocating-sliding wear behavior of nanostructured and ultra-fine high-silicon bainitic steels. *Wear* **2015**, *202*, 338–339.

31. Liu, W.; Qu, J.; Shao, H. A study of bainitic nodular cast iron for grinding balls. *J. Mater. Sci.* **1997**, *32*, 427–430.

32. Rementeria, R.; Morales, L.; Kuntz, M.; Garcia-Mateo, C.; Kerscher, E.; Sourmail, T.; Caballero, F.G. On the role of microstructure in governing the fatigue behavior of nanostructured bainitic steels. *Mater. Sci. Eng. A* **2015**, *630*, 71–77.

33. Garcia-Mateo, C.; Mathew, P.; Caballero, F.G.; Bhadeshia, H.K.D.H. Tempering of hard mixture of bainitic ferrite and austenite. *Mater. Sci. Tech.* **2004**, *20*, 814–818.

34. Caballero, F.G.; Miller, M.K.; Garcia-Mateo, C.; Capdevila, C.; Babu, S.S. Redistribution of alloying elements during tempering of a nanocrystalline steel. *Acta Mater.* **2008**, *56*, 188–199.

35. Pujante, J.; Casellas, D.; Sourmail, T.; Caballero, F.G.; Soto, A.; Llanos, J.M.; Vuorinen, E.; Prakash, B.; Hardell, J.; Moghaddam, P.V.; et al. *Novel Nano-Structured Bainitic Steels for Enhanced Durability of Wear Resistant Components: Microstructural Optimisation through Simulative Wear and Field Tests. BAINWEAR.* Research Programme of the Research Fund for Coal and Steel, European Commission, Brussels, Belgium, 2018, in press.